Surface Waves in Laterally Heterogeneous Media

Samuel Bignardi[1]; Francesco Fedele[2]; Giovanni Santarato[3]; Anthony J. Yezzi[4]; and Glenn J. Rix[5]

Abstract: Surface wave methods exploit the dispersive properties of Rayleigh and Love waves to estimate the shear wave velocity profiles in vertically heterogeneous subsurfaces. Typically, they rely on a simplified one-dimensional (1D) analytical forward model where the lateral variation of the layer thickness is neglected and so is the fraction of the incident energy of the fundamental mode that is reflected or converted to higher modes. A theoretical study is presented that attempts to define an analytical model that overcomes the limitations of 1D forward models. In particular, we revisit properties of semianalytical approaches that aim at solving the dynamics of Love waves in laterally heterogeneous media made of a soft upper layer of varying thickness lying over an infinitely deep hard layer. The novel analytical model stems from a local-mode expansion of waves with laterally varying amplitudes, which allows for both reflections of the incident modes and coupling to higher modes. The best wave approximation stems from an action principle that leads to a coupled system of second-order ordinary differential equations (ODEs) for the wave amplitudes. Last, an application of this model and its validity are discussed. **DOI: 10.1061/(ASCE)EM.1943-7889.0000566.**

CE Database subject headings: Surface waves; Mathematical models; Layered systems; Heterogeneity.

Author keywords: Surface waves; Mathematical model; Layered systems; Lateral heterogeneity; Spectral method; Lagrangian minimization.

Introduction

The dispersive nature of Rayleigh and Love waves in a heterogeneous half-space is exploited in surface methods to obtain the shear wave velocity profile from the surface wave particle motions excited and recorded on the ground surface (that is, the boundary of the medium). The solution of the inverse problem to obtain the shear wave velocity (and/or material damping ratio) profile requires a forward (subsurface) model to predict the propagation, scattering, and dissipation of seismic waves in the medium. One widely used forward model in surface wave testing is that in which each layer is isotropic and homogeneous, and the layer interfaces are planar and horizontal. The key properties of each layer are the elastic parameters (or seismic wave velocities), the mass density, and the thickness. Such models are capable of capturing only the vertical variation in elastic properties—that is, they are one dimensional (1D). One of the attractive features of this model is that it is very computationally efficient to calculate the modal displacements and stresses using matrix operations (Aki and Richards 2002), which makes it ideal for inverse problems employing iterative solutions. Clearly, however, this model is only an approximation of the actual soil conditions for most sites, and its use may lead to misleading results if the actual soil profile is far from the assumed geometry. Indeed, lateral variation and wave backscattering are not taken into account, and only a few higher modes of vibration are considered. The spatial variation of the layer thickness is usually neglected and so is the fraction of incidental energy of the fundamental mode that is reflected or converted to higher modes. In this paper, an analytical study is presented that aims at modeling elastic waves in laterally varying media that overcomes the limitations of traditional 1D forward models. The numerical alternative based on the boundary element method (Brebbia et al. 1984) is discussed elsewhere (Bignardi et al. 2012; Bignardi 2011). Hereafter, the focus is on the dynamics of Love waves, which are attractive from a theoretical point of view and have been studied analytically by several authors (Noyer 1961; Knopoff and Mal 1967; Wolf 1970; Lysmer and Drake 1971; Gjevik 1973; Maupin 2007; Hador and Buchen 1999). Studies on the wave dynamics in laterally varying media span at least 40 years of literature, and several methods have been formulated. Among these, the Lagrangian approach was introduced by Whitham (1967, 1974) to investigate the dynamics of nonlinear water waves. Applications of such a variational method to the study of long seismic waves were presented by Gjevik (1973) and Hador and Buchen (1999) for Love and Rayleigh waves, respectively. On the other hand, analytical methods that exploit the coupling and matching of different wave modes have been proposed by Maupin and Kennett (1987) and Maupin (1992) (see also Maupin 2007 for a review of such methods).

In particular, the analytical model in Maupin (1988) is valid for Rayleigh and Love waves, and for structures that have several layers and lateral variations of the elastic properties inside the layers. Later, Maupin (1992) extended the coupling method to waves that propagate at an angle to the two-dimensional (2D) structure and to inelastic media. Other analytical approaches based on the Jeffreys, Wentzel, Kramers, and Brillouin (JWKB) approximation find approximate solutions of the elastic equations with spatially varying coefficients. For example, Tromp and Dahlen (1992) derived local

[1]Research Fellow, Dept. of Physics and Earth Sciences, Univ. of Ferrara, Via Saragat 1, Building B-206, 44122 Ferrara, Italy (corresponding author). E-mail: sedysen@gmail.com

[2]Associate Professor, School of Civil and Environmental Engineering and School of Electrical and Computer Engineering, Georgia Institute of Technology, 777 Atlantic Dr. N.W., Atlanta, GA 30332-0250.

[3]Associate Professor, Dept. of Physics and Earth Sciences, Univ. of Ferrara, Via Saragat 1, Building B-206, 44122 Ferrara, Italy.

[4]Ken Byers Professor, School of Electrical and Computer Engineering, Georgia Institute of Technology, 777 Atlantic Dr. N.W., Atlanta, GA 30332-0250.

[5]Professor and Associate Chair for Finance and Administration, School of Civil and Environmental Engineering, Georgia Institute of Technology, 790 Atlantic Dr., Atlanta, GA 30332-0355.

Note. This manuscript was submitted on December 13, 2011; approved on November 7, 2012; published online on August 15, 2013. Discussion period open until February 1, 2014; separate discussions must be submitted for individual papers. This paper is part of the ***Journal of Engineering Mechanics***, Vol. 139, No. 9, September 1, 2013. ©ASCE, ISSN 0733-9399/2013/9-1158–1165/$25.00.

Love and Rayleigh eigenfunctions, local dispersion relations, and transport equations, which determine the wave propagation on a smooth, laterally heterogeneous Earth model. Clearly, in geophysical imaging, numerical modeling of elastic waves has become popular in the last two decades or so (Virieux et al. 2011). However, analytical approaches are still valuable for fast computations of the wave propagation when the source is far from the investigated region (see, for example, Panza et al. 2001) or in some full waveform inversion methods (see, for example, Du 2002).

In this paper, it is proposed to revisit semianalytical approaches with their advantages and limitations by presenting an analytical model that stems from a novel local-mode representation of monochromatic Love waves, which is optimized by an action principle. To do so, conservative systems are studied, and the dynamic equations follow from a variational principle based on the Lagrangian for Love waves (Gjevik 1973). Consider a homogeneous upper soft layer with varying thickness $\eta(x)$ lying over a semi-infinite hard layer, with x as the horizontal axis, as shown in Fig. 1. The vertical profile of wave displacements at any horizontal position x is represented by a local-mode series involving the propagating eigenmodes allowed by the dispersion relation, which depends on the local thickness $\eta(x)$. The proposed eigenmode series expansion accounts for both forward-propagating and backward-propagating waves. Locally, such eigenmodes are exactly equal to those for a parallel-layered media, but their wavelength is spatially varying because the local thickness of the layer is. They satisfy the zero-stress condition at the free surface and the continuity of the vertical stresses at the interface between the two layers. The amplitudes of the Love eigenmodes are unknown and are assumed to be spatially varying in x. Then, exploiting an action principle, the associated Euler-Lagrange equations yield a set of coupled second-order ordinary differential equations (ODEs) for the optimal amplitudes that satisfy the wave dynamics. To the present authors' knowledge, such formulation has not yet been applied to problems in seismic wave propagation. It may be a useful contribution because the proposed model considers a laterally varying layered geometry with constant elastic parameters, a special case of the more general model derived by Maupin (1988).

The paper is structured as follows: First, the theoretical formulation for Love wave is introduced. Then, the associated variational formulation based on the Lagrangian is presented. A local-mode wave expansion is defined and the associated coupled-mode system follows from an action principle via the Euler-Lagrange equations. Last, applications and limitations of the proposed model will be discussed.

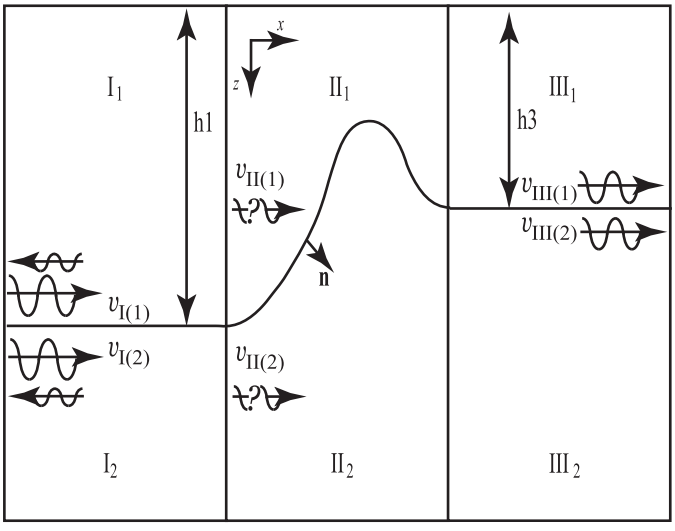

Fig. 1. Model setup and geometry of laterally varying two-layered media

Transmission Problem

Consider a laterally heterogeneous medium such as that shown in Fig. 1, where x and z are, respectively, a horizontal and a vertical coordinate. Let the upper and the lower layers have densities ρ_1 and ρ_2, respectively. The upper layer has a free boundary at $z = 0$, and the lower layer is assumed to be infinitely deep. The media is divided in three vertical zones: I ($x < -L$), II ($-L \le x \le L$), and III ($x > L$), respectively. The two layers extend horizontally to infinity, and in the far-field zones I and III the layers are parallel. In the intermediate zone II, the upper and lower layer are separated by a varying interface $z = \eta(x)$. Zone I is excited by an incident monochromatic plane wave that generates a displacement field $v_{in}(x, z, t)$ that propagates in the x-direction. As it passes through zone II, it undergoes reflections, and only part of its energy is transmitted to zone III, where the wave displacements $v_{III}(x, z, t)$ propagate undisturbed. The cumulated effect of all the reflections in zone II yields a reflected back-propagating wave with displacements $v_R(x, z, t)$ through zone I, and the total wave field in zone I is $v_I = v_R + v_{in}$. The displacements of these waves are normal to the plane through the x-axis and z-axis. If the materials in both layers behave according to linear elastic laws, then the displacements in zone II vary according to the equations of motion (Aki and Richards 2002)

$$-\rho \frac{\partial^2 v_{II}}{\partial t^2} + \mu \nabla^2 v_{II} = 0 \tag{1}$$

where $\nabla = \partial_x \hat{\mathbf{x}} + \partial_z \hat{\mathbf{z}}$; $\hat{\mathbf{x}}$, $\hat{\mathbf{z}}$ = unit vectors of x and z; ρ and μ are soil parameters given by the piecewise functions

$$\rho(x,z) = \begin{cases} \rho_1, & 0 \le z \le \eta(x) \\ \rho_2, & z > \eta(x) \end{cases}, \quad \mu(x,z) = \begin{cases} \mu_1, & 0 \le z \le \eta(x) \\ \mu_2, & z > \eta(x) \end{cases}$$

At the free-surface $z = 0$, and at $z \to \infty$ zero-stress boundary conditions are imposed, viz

$$\mu \frac{dv_{II}}{dz}\bigg|_{z=0} = 0, \quad \mu \frac{dv_{II}}{dz}\bigg|_{z\to\infty} = 0 \tag{2}$$

The continuity of both displacements and normal stresses at the interface $z = \eta(x)$ requires that

$$[v_{II}]_{z=\eta} = 0, \quad \left[\mu \nabla v_{II} \cdot \hat{\mathbf{n}}\right]_{z=\eta} = 0 \tag{3}$$

where $[q]_{z=\eta}$ stands for the jump of $q(z)$ across $z = d$, that is

$$[q]_{z=d} = \lim_{\epsilon \to 0} [q(z+\epsilon) - q(z-\epsilon)] \tag{4}$$

and $\hat{\mathbf{n}}$ is the unit vector normal to the interface η, defined as

$$\hat{\mathbf{n}} = \frac{1}{\sqrt{1 + \left(\frac{d\eta}{dx}\right)^2}} \left(-\frac{d\eta}{dx}\hat{\mathbf{x}} + \hat{\mathbf{z}}\right) \tag{5}$$

J. Eng. Mech. 2013.139:1158-1165.

The continuity of stresses and displacements at the common boundaries of zones I–II ($x = -L$) and zones II–III ($x = L$), requires the following matching conditions

$$\begin{aligned} &(v_{II} - v_I)|_{x=-L} = 0, \quad \mu\left(\frac{\partial v_{II}}{\partial x} - \frac{\partial v_I}{\partial x}\right)\Big|_{x=-L} = 0 \\ &(v_{III} - v_{II})|_{x=L} = 0, \quad \mu\left(\frac{\partial v_{III}}{\partial x} - \frac{\partial v_{II}}{\partial x}\right)\Big|_{x=L} = 0 \end{aligned} \tag{6}$$

It is straightforward to prove that the boundary value problem [Eqs. (1)–(3) and (6)] is the minimizer of an action $\mathcal{A}$ that follows from $\delta\mathcal{A} = 0$, where δ denotes variational differentiation (see Appendix I). In particular, $\mathcal{A}$ is given by

$$\mathcal{A} = \int_{t_1}^{t_2} \int_{-L}^{L} \mathcal{L}\, dx\, dt \tag{7}$$

where the Lagrangian density is defined as

$$\mathcal{L} = \mathcal{T} - \mathcal{K} - \mathcal{B} \tag{8}$$

Here, $\mathcal{J}$ and $\mathcal{K}$ are the kinetic and potential energy densities given, respectively, by

$$\mathcal{J} = \frac{1}{2}\int_0^\infty \rho\left(\frac{\partial v_{II}}{\partial t}\right)^2 dz, \quad \mathcal{K} = \frac{1}{2}\int_0^\infty \mu|\nabla v_{II}|^2 dz \tag{9}$$

The term $\mathcal{B}$ accounts for the matching and boundary conditions [Eqs. (2), (3), and (6)] as

$$\begin{aligned} \mathcal{B} = {} & [\mu\, v_{II}]_{z=\eta}\left(\frac{\partial v_{II}}{\partial z} - \frac{\partial v_{II}}{\partial x}\frac{d\eta}{dx}\right)\Big|_{z=\eta} \\ & - \int_0^\infty \mu\frac{\partial v_I}{\partial x}\left(v_{II} - \frac{v_I}{2} - v_{in}\right)\Big|_{x=-L} dz \\ & + \int_0^\infty \mu\frac{\partial v_{III}}{\partial x}\left(v_{II} + \frac{v_{III}}{2}\right)\Big|_{x=L} dz \end{aligned} \tag{10}$$

In the following, a local-mode expansion of the wave field for the laterally varying medium of Fig. 1 is introduced. Then, the equations governing the wave dynamics are derived by minimizing the action [Eq. (7)].

Wave Expansion and Dynamics

Mode Expansion for Zones I and III

Assume the thickness of the upper layer equal to d. The standard representation of the wave field v_p is given in the form

$$v_p(x, z, t) = \sum_n A_n f_n(z; d) e^{i(k_n x - \omega t)} + c.\,c. \tag{11}$$

where $c.\,c.$ denotes complex conjugation; the wave numbers k_n satisfy the dispersion relation

$$\tan(i\nu_1 d) = -\frac{\mu_2\nu_2}{i\mu_1\nu_1}, \quad \nu_i = \sqrt{k^2 - \frac{\rho_i\omega^2}{\mu_i}} = \sqrt{k^2 - \frac{\omega^2}{\beta_i^2}} \tag{12}$$

and $f_n(z;\, d)$ are the eigenfunctions of the Sturm-Liouville problem

$$\frac{d^2 f_n}{dz^2} - \nu_i^2 f_n = 0 \tag{13}$$

with the requirements of continuity for both displacements and vertical stresses at $z = d$, viz

$$[f_n]_{z=d} = 0, \quad \left[\mu\frac{df_n}{dz}\right]_{z=d} = 0 \tag{14}$$

and zero-stresses at the free-surface, viz

$$\frac{df_n}{dz}\Big|_{z=0} = 0 \tag{15}$$

From Eq. (11), the incident and reflected components of the displacements $v_I = v_{in} + v_R$ in zone I can be defined, respectively, as

$$\begin{aligned} v_{in} &= \sum_n I_n e^{ik_{n_I}(x+L)} f_n(z; d_1) e^{-i\omega t} + c.\,c. \\ v_R &= \sum_n R_n e^{-ik_{n_I}(x+L)} f_n(z; d_1) e^{-i\omega t} + c.\,c. \end{aligned} \tag{16}$$

where $d_1 = \eta(-L)$; and I_n and R_n = constant amplitudes. Further, in zone III v_{III} is defined as

$$v_{III} = \sum_n T_n e^{ik_{n_{III}}(x-L)} f_n(z; d_3) e^{-i\omega t} + c.\,c. \tag{17}$$

where $d = d_3 = \eta(L)$; and T_n = amplitude of the transmitted wave. The wave expansion for zone II requires a new formulation, as subsequently discussed.

Local-Mode Wave Representation for Zone II

The spatially varying wave field in zone II can be efficiently represented by the local-modes series [Eq. (18)], as in Maupin (2007),

$$v_{II}(x, z, \omega) = \sum_n a_n(x) f_n(z, \omega, \eta) e^{i\left[\int_0^x k_{n_{II}}(\omega,\xi)d\xi - \omega t\right]} + c.\,c. \tag{18}$$

where a_n = unknown spatially varying amplitudes, and the integral in the exponential term allows us to follow the phase evolution of the wave field.

Because the depth $d = \eta(x)$ is spatially varying, so are both $k_n(x)$ and $f_n(z,\, \eta)$. Consequently, the Sturm-Liouville problem [Eq. (13)] can be considered as a continuous family of problems with parameter $d = \eta(x)$. This suggests the equivalent representation

$$v_{II}(x, z, t) = \sum_n A_n(x) f_n(z, \eta) e^{i\left[k_{n_{II}}(x)\, x - \omega t\right]} + c.\,c. \tag{19}$$

where now amplitudes A_n are complex and related to a_n and the associated phases by

$$a_n(x) = A_n(x) e^{i\left[-\int_{-L}^x k_{n_{II}}(\xi)d\xi + k_{n_{II}}(x)x\right]} \tag{20}$$

J. Eng. Mech. 2013.139:1158-1165.

Clearly, the complex amplitude A_n describes both the forward-propagating and the backward-propagating modes and its evolution reflects the coupling between modes, the reflection, and the phase adjustment of the modes themselves. The advantage of the compact representation [Eq. (19)] is that the associated dynamical equations for A_n, as will be shown later, are a set of N second-order ODEs that will be solved using spectral methods. Splitting A_n in the two backward and forward waves would lead to a set of 2N first-order ODEs. The spectral method used in this work is more efficient and accurate for second-order ODEs.

Note that Eq. (19) satisfies the continuity of displacements at the interface because $[f_n]_{z=\eta} = 0$ at any x, but the normal stresses are not continuous. Indeed, from Eqs. (19) and (14)

$$\left[\mu \nabla v_{II} \cdot \hat{\mathbf{n}}\right]_{z=\eta} = -\frac{d\eta}{dx}\left[\mu \frac{\partial v_{II}}{\partial x}\right]_{z=\eta} \tag{21}$$

As a consequence, the total energy density $\mathcal{E} = \mathcal{J} + \mathcal{K}$ is also not conserved along x. However, the local-mode representation [Eqs. (16), (17), and (19)]

$$\begin{aligned} v_I &= \sum_n \left(I_n e^{ik_{n_I}(x+L)} + R_n e^{-ik_{n_I}(x+L)}\right) f_n(z;d_1) e^{-i\omega t} + c.c. \\ v_{II} &= \sum_n A_n(x) f_n(z;x) e^{i\left[k_{n_{II}}(x)x - \omega t\right]} + c.c. \\ v_{III} &= \sum_n T_n e^{ik_{n_{III}}(x-L)} f_n(z;d_3) e^{-i\omega t} + c.c. \end{aligned} \tag{22}$$

can be optimized by the action principle to minimize the residual [Eq. (21)]. Indeed, given the incident amplitude I_n, we seek the optimal functions $A_n(x)$, the reflection and transmitted coefficients R_n and T_n that minimize the action $\mathcal{A}(A_n, R_n, T_n)$ in Eq. (8), as follows:

$$\frac{\delta \mathcal{A}}{\delta A_n} = \frac{\delta \mathcal{A}}{\delta T_n} = \frac{\delta \mathcal{A}}{\delta R_n} = 0 \tag{23}$$

where δ denotes variational differentiation. In particular, the first variation in Eq. (23) yields a coupled system of second-order ODEs) for A_n as

$$\sum_{j=1}^{M} b_{ij}\frac{d^2 A_j}{dx^2} + c_{ij}\frac{dA_j}{dx} + d_{ij}A_j = 0, \quad i = 1, \ldots, M \tag{24}$$

and the boundary conditions at $x = -L$ and $x = L$, respectively, as

$$2ik_n I_n = \left(2ik_n A_n + \frac{dA_n}{dx}\right)\Big|_{x=-L} e^{-ik_n L}, \quad \frac{dA_n}{dx}\Big|_{x=L} = 0 \tag{25}$$

The matrix elements b_{ij}, c_{ij}, and d_{ij} are given in Appendix II. Further, the other two variations in Eq. (23) yield the reflection and transmitted coefficients, which depend upon the mode amplitudes A_n, such as

$$R_n = e^{-ik_n L}A_n\big|_{x=-L} - I_n, \quad T_n = A_n\big|_{x=L} e^{ik_n L} \tag{26}$$

The set of Eq. (24) together with the boundary conditions [Eq. (25)] are solved numerically via standard Chebyshev spectral methods. We refer to Trefethen (2000) for details on the numerical implementation of the spectral solver. For a flat interface, the model [Eq. (24)] decouples, and the classical solution for Love waves is recovered (Aki and Richards 2002). Indeed, to assess the reliability of the algorithm, several tests were performed for a geometry with parallel layers, for which the solver yielded wave amplitudes constant in the x direction, as expected.

Note that backreflections are taken into account by the analytical model [Eq. (24)]. This is because the amplitudes A_n are complex-valued solutions of second-order ODEs that provide for the displacements v_{II} a solution in the form of two opposite traveling waves. Last, observe that Love eigenmodes are independent locally but not globally, and mode coupling is necessary to satisfy both matching and boundary conditions on the laterally varying interface.

Applications

Consider the two-layered subsurface shown in Fig. 2. For the upper (lower) layer, $\rho_1 = 1{,}600$ (2,400) kg/m^3 and $\beta_1 = 400$ (1,500) m/s. The varying interface is modeled by a half-sine-shaped buried hill with average 10% slope over a depth $H = 1.2$ km, and the spatial extension is $2L = 6$ km. Waves propagate in the x-direction at $f = \omega/2\pi = 8$ Hz. At this frequency, in addition to the fundamental mode, with wavelength $L_0 = 314.8$ m, six higher modes are admissible with wavelengths $L_1 = 320.4$ m, $L_2 = 332.4$ m, $L_3 = 353.2$ m, $L_4 = 388.2$ m, $L_5 = 451.2$ m, and $L_6 = 591.4$ m, respectively. For simplicity, in the present application we consider a setup with a constant number of modes in zone II. The case of subregions with different numbers of modes will not be considered here; however, such configurations can be handled by the proposed approach by splitting the computational domain into subregions with a fixed number of modes and then matching the solutions by imposing continuity of displacements and stresses. All the modes are set to have identical amplitudes $A_0 = 0.005$ m and zero phases at $x = -L$. From Eq. (22), each eigenmode in zone II can be written as

$$|A_n| f_n(z,\eta)\exp[i(\theta_n + k_{n_{II}}x - \omega t)] \tag{27}$$

where $|A_n|$ and $\theta_n = \arctan[\mathrm{Im}(A_n)/\mathrm{Re}(A_n)]$ are the absolute value and the phase of the complex amplitude A_n, respectively. Then, after solving the ODE system [Eq. (24)], the local wave number k_n of each mode can be computed from Eq. (27) as

$$k_n(x) = \tilde{k}_n(x) + x\frac{dk_n}{dx} + \frac{d\theta_n}{dx} \tag{28}$$

where $\tilde{k}_n(x) = k_{n_{II}}$ is the local approximation computed from the dispersion relation [Eq. (12)], with d as the interface depth $\eta(x)$. The associated phase velocity C_n follows as

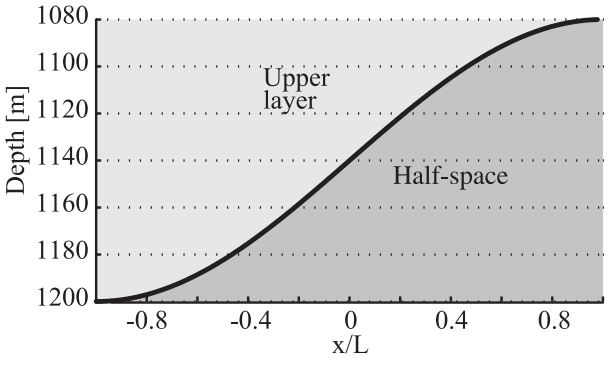

Fig. 2. Two-layered media with varying interface modeled by a half-sine-shaped buried hill with average 10% slope over a depth $H = 1.2$ km, and spatial extension $2L = 8$ km; for the upper (lower) layer, $\rho_1 = 1{,}600$ (2,400) kg/m^3, and $\beta_1 = 400$ (1,500) m/s

J. Eng. Mech. 2013.139:1158-1165.

$$C_n(x) = \frac{\omega}{k_n(x)} \tag{29}$$

Fig. 3 shows the spatial variation of the magnitude of the complex amplitudes A_n/A_0 at $x = -L$. Note the amplification of higher modes in the region where the thickness of the upper layer decreases. This is expected because of the redistribution of energy among the modes, which is approximately conserved. Indeed, we were able to investigate interface slopes $< 10\%$ with a negligible loss in energy. However, for interfaces with 15% slope, the energy loss increases to 5%. Larger slopes up to 25% yield 15% of the energy loss. Fig. 4 shows also the lateral variation of the wave number k_n in the x-direction (bold lines) in comparison with the local approximation $\tilde{k}_n$. Note that the wave number of the fundamental mode does not vary laterally and is almost equal to that of horizontal shear waves in the upper layer (dashed lines). Indeed, its wavelength $L_0 = 314.8$ m is smaller than the average interface depth H, and the fundamental mode is not affected by the interface. However, lateral inhomogeneities affect the lowermost higher modes, whose wave numbers tend to increase as they propagate over shallower regions of the upper layer, shortening their wavelengths. As a consequence, for higher modes the phase velocity C_n increases in comparison with the associated parallel-layered counterpart ω/k_n (see Fig. 5). Fig. 6 shows the spatial variation of the wave displacements v_{II} (bold line) at the free surface ($z = 0$) and the associated parallel-layered counterpart $(v_{II})_p$ (dashed line), computed as if the layers were parallel, with $d = \eta(-L) = 1{,}200$ m, as follows:

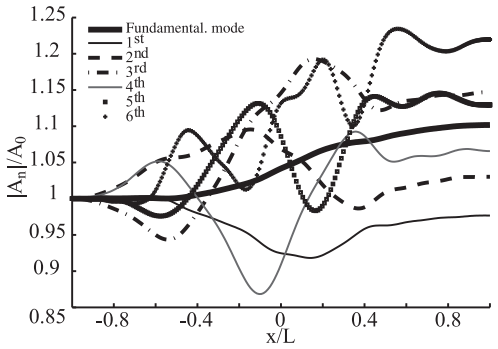

Fig. 3. Spatial variation of normalized eigenmode amplitudes $|A_n|/A_0$ for the two-layered media in Fig. 2 ($f = 8$ Hz)

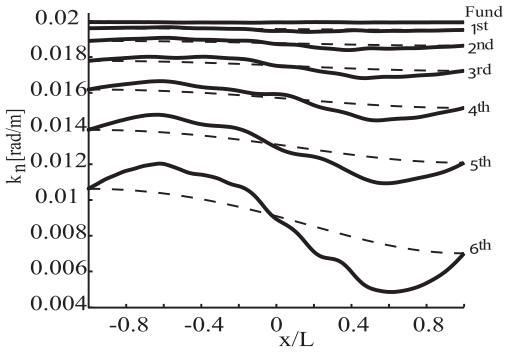

Fig. 4. Spatial variation of the wave number k_n (bold lines) and the associated approximation $\tilde{k}_n = k_{n_{II}}$ (dashed lines) from the dispersion relation [Eq. (12)], with d as the interface depth $\eta(x)$, for the two-layered media in Fig. 2 ($f = 8$ Hz)

$$(v_{II})|_{z=0} = \sum_n A_n(x) f_n(0,\eta) e^{i\left[k_{n_{II}}(x)x - \omega t\right]}$$

$$(v_{II})_p\Big|_{z=0} = \sum_n A_0 f_n(0,\eta) e^{i\left[k_{n_{II}}(-L)x - \omega t\right]}$$

Because all the modes are in phase, constructive interference (linear focusing) occurs at $x/L = 0$ in the parallel-layered case. Such focusing is annihilated when waves propagate through the laterally varying media from deep to shallow areas, reducing displacements because of the increased stiffness of the first layer. The associated power spectra $S(k)$ and $S_p(k)$ for v_{II} and $(v_{II})_p$ at the free surface are shown in Fig. 7, respectively. The spectrum S is wider than S_p, as expected, mainly because of the fact that the modes have laterally varying $k_{n_{II}}$, and backreflections and mode coupling may have a minor role. Last, as previously stated, we observed energy losses $> 15\%$ for slopes $> 15\%$. Indeed, the analytical model [Eq. (24)], although derived from an action principle, is inadequate to correctly represent the wave field near the interface η because of errors in the stress-matching boundary conditions at the interface [see Eq. (21)]. Such stress mismatch is an indirect indication that the wave energy is not conserved. To minimize energy losses, Rutherford and Hawker (1981) proposed expanding the wave field using perturbed local modes that satisfy the continuity conditions at the interface to the first order in the slope. On the other hand, Maupin (1988) transformed the traction discontinuity along the interface in volume forces to satisfy

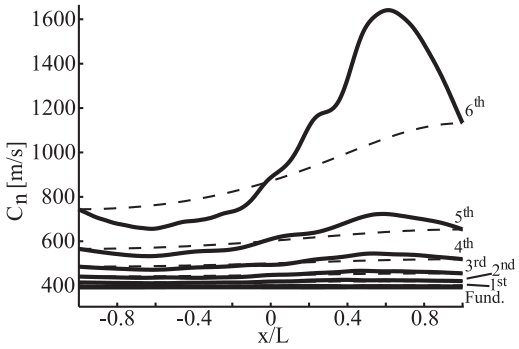

Fig. 5. Phase velocity C_n (bold lines) and the associated local approximation $\tilde{C}_n(x) = \omega\tilde{k}_n$ (dashed lines) computed from the dispersion relation [Eq. (12)], with d as the interface depth $\eta(x)$ for the two-layered media in Fig. 2 ($f = 8$ Hz)

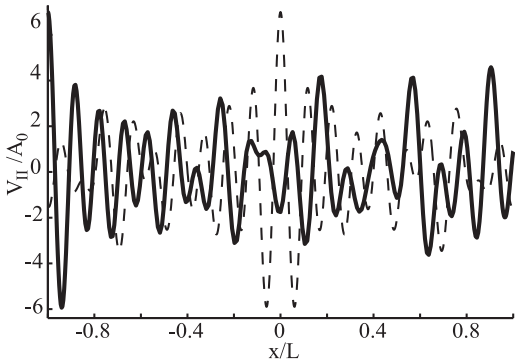

Fig. 6. Normalized wave displacements v_{II}/A_0 (bold line) at the surface ($z = 0$) for the two-layered media in Fig. 2 and the associated parallel-layered counterpart (dashed line)

J. Eng. Mech. 2013.139:1158-1165.

stress continuity. The proposed solution of the wave field of zone II that follows from solving the Euler-Lagrange [Eqs. (24) and (25)], is optimal in the sense that the error associated with the continuity of the normal stresses $\tau_n = \mu \nabla v_{II} \cdot \hat{\mathbf{n}}$ across η is the lowest possible. Fig. 8 shows the spatial variation of the dimensionless stress jump $[\tau_n]/\max(\tau_n)_1$ across η for different slopes, with $\max(\tau_n)_1$ as the maximum normal stress at η in the upper layer. As one can see, only for slopes greater than 10%, the jumps are not negligible, and as a consequence the variational solution is not reliable. To provide a simple explanation of the limitated optimality of the proposed Lagrangian model, consider the general solution of the elastic Navier's equations. It can be obtained via separation of variables (Aki and Richards 2002) as the linear superposition of two plane S waves traveling along z in opposite direction, as follows:

$$v \approx \left(A_n e^{i k_{z_n} z} + B_n e^{-i k_{z_n} z}\right) e^{i\left[k_{n_{II}}(x) x - \omega t\right]} \tag{30}$$

where $k_n = \sqrt{k_{x_n}^2 + k_{z_n}^2}$ (Aki and Richards 2002). If the free surface is flat, to satisfy the zero-stress condition at $z = 0$ one must have $B_n = A_n$, and

$$v \approx A_n \left(e^{i k_{z_n} z} + e^{-i k_{z_n} z}\right) e^{i\left[k_{n_{II}}(x) x - \omega t\right]} = A_n \cos(k_{z_n} z) e^{i\left[k_{n_{II}}(x) x - \omega t\right]} \tag{31}$$

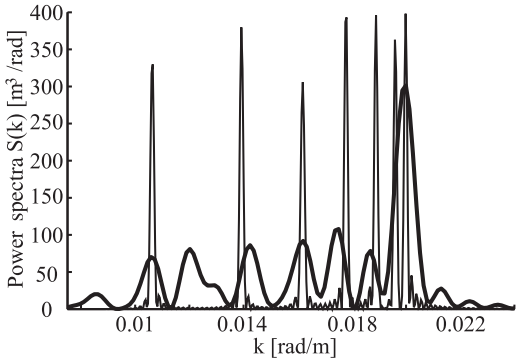

Fig. 7. Power spectra $S(k)$ of the surface displacements in zone II (bold line) and the associated parallel-layered counterpart for the two-layered media in Fig. 2 ($f = 8$ Hz)

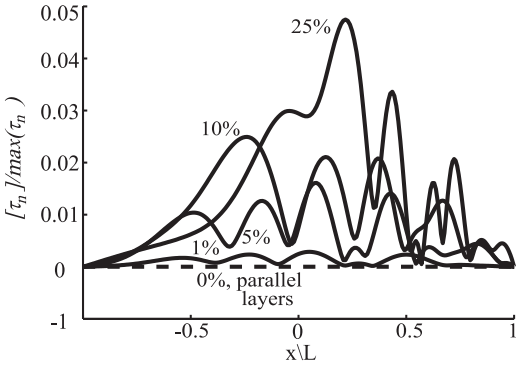

Fig. 8. Spatial variation of the normal stress jump τ_n across the interface for different slopes with $\tau_n = \mu \nabla v_{II} \cdot \hat{n}$; $\max(\tau_n)_1$ is the maximum stress at the interface in the upper layer ($f = 8$ Hz)

If the interface has weak to moderate slopes, the two S waves have similar wave numbers k_{z_n}, and their constructive interference can be modeled by Eq. (31) along with the minimization of the associated action, which can compensate for the stress mismatch at the interface. When the interface has large slopes ($>15\%$), the two S waves have different values of k_{z_n}, and the original elastic partial differential equations (PDEs) cannot be solved by separation of variables in the x and z directions. In this case, the set of local Love eigenmodes of Eq. (31) is not suitable to represent independent S waves, and the Lagrangian minimization partially compensates for the mismatch. Work is in progress to satisfy the stress continuity at the interface by including fictitious volume forces in the present variational model, as is done in Maupin (1988), and thus to provide comparisons with the more general Maupin's formulation, which is valid for multilayered geometries and varying elastic parameters within the layers.

Conclusions

Semianalytical approaches have been revisited to solve for the propagation of Love waves in laterally heterogeneous media. To do so, a novel analytical model based on a local-mode representation of the surface displacements is formulated. Such ansatz is exact for a flat interface, and it is a good approximation for weakly varying sloping interfaces (Gjevik 1973). The proposed Lagrangian minimization extends the applicability of this ansatz to interfaces with moderate slopes, and it accounts for backreflections and higher-mode coupling. However, for steep interfaces $>15\%$, the proposed local-mode representation [Eq. (19)] is poor because it does not accurately model reflections at both the interface and the free surface. Work is in progress to improve the proposed variational model by transforming the traction discontinuity along the interface in volume forces, as in Maupin (1988), and will be discussed elsewhere.

Appendix I. Action Principle for Love Waves

The Lagrangian [Eq. (8)] is explicitly given by

$$\begin{aligned}\mathcal{L} = {} & \frac{1}{2}\int_0^{\eta(x)} \rho_1 \left(\frac{\partial v_{1_{II}}}{\partial t}\right)^2 - \mu_1 \left[\left(\frac{\partial v_{1_{II}}}{\partial x}\right)^2 + \left(\frac{\partial v_{1_{II}}}{\partial z}\right)^2\right] dz \\ & + \frac{1}{2}\int_{\eta(x)}^{\infty} \rho_2 \left(\frac{\partial v_{2_{II}}}{\partial t}\right)^2 - \mu_2 \left[\left(\frac{\partial v_{2_{II}}}{\partial x}\right)^2 + \left(\frac{\partial v_{2_{II}}}{\partial z}\right)^2\right] dz \\ & - \mu_2 \left(\frac{\partial v_{2_{II}}}{\partial z} - \frac{\partial v_{2_{II}}}{\partial x}\frac{\partial \eta_{(x)}}{\partial x}\right)(v_{2_{II}} - v_{1_{II}})\Big|_{z=\eta_{(x)}} \\ & + \int_0^{\infty} \mu \frac{\partial v_I}{\partial x}(v_{II} - 1/2 v_I - v_{in})\Big|_{x=-L} dz \\ & - \int_0^{\infty} \mu \frac{\partial v_{III}}{\partial x}(v_{II} + 1/2 v_{III})\Big|_{x=L} dz\end{aligned}$$

where the subscripts 1 and 2 denote the upper and lower media, respectively. Variational differentiation of action $\mathcal{A}$ yields

J. Eng. Mech. 2013.139:1158-1165.

$$\delta\mathcal{A} = \delta \int_{t_1}^{t_2}\int_{\Omega} \mathcal{L}\, d\Omega\, dt$$

$$= + \int_{t_1}^{t_2}\int_{x_1}^{x_2}\int_{0}^{\eta_{(x)}} \rho_1 \frac{\partial v_{1_{II}}}{\partial t}\frac{\partial}{\partial t}\delta v_{1_{II}} - \mu_1\left(\frac{\partial v_{1_{II}}}{\partial x}\frac{\partial}{\partial x}\delta v_{1_{II}} + \frac{\partial v_{1_{II}}}{\partial z}\frac{\partial}{\partial z}\delta v_{1_{II}}\right) dz\, dx\, dt$$

$$+ \int_{t_1}^{t_2}\int_{x_1}^{x_2}\int_{\eta_{(x)}}^{\infty} \rho_2 \frac{\partial v_{2_{II}}}{\partial t}\frac{\partial}{\partial t}\delta v_{2_{II}} - \mu_2\left(\frac{\partial v_{2_{II}}}{\partial x}\frac{\partial}{\partial x}\delta v_{2_{II}} + \frac{\partial v_{2_{II}}}{\partial z}\frac{\partial}{\partial z}\delta v_{2_{II}}\right) dz\, dx\, dt$$

$$- \int_{t_1}^{t_2}\int_{x_1}^{x_2} \mu_2\left(\frac{\partial}{\partial z}\delta v_{2_{II}} - \frac{\partial}{\partial x}\delta v_{2_{II}}\frac{\partial \eta_{(x)}}{\partial x}\right)(v_{2_{II}} - v_{1_{II}})\Big|_{z=\eta} dx\, dt$$

$$- \int_{t_1}^{t_2}\int_{x_1}^{x_2} \mu_2\left(\frac{\partial v_{2_{II}}}{\partial z} - \frac{\partial v_{2_{II}}}{\partial x}\frac{\partial \eta_{(x)}}{\partial x}\right)(\delta v_{2_{II}} - \delta v_{1_{II}})\Big|_{z=\eta} dx\, dt$$

$$+ \int_{t_1}^{t_2}\int_{0}^{\infty} \mu \frac{\partial v_I}{\partial x}\left(\delta v_{II} - \frac{1}{2}\delta v_I - \delta v_{in}\right)\Big|_{x=-L} dz$$

$$+ \int_{t_1}^{t_2}\int_{0}^{\infty} \mu \frac{\partial \delta v_I}{\partial x}\left(v_{II} - \frac{1}{2} v_I - v_{in}\right)\Big|_{x=-L} dz$$

$$+ \int_{t_1}^{t_2}\int_{0}^{\infty} \mu \frac{\partial v_{III}}{\partial x}\left(\delta v_{II} - \frac{1}{2}\delta v_{III}\right)\Big|_{x=L} dz$$

$$- \int_{t_1}^{t_2}\int_{0}^{\infty} \mu \frac{\partial \delta v_{III}}{\partial x}\left(v_{II} + \frac{1}{2} v_{III}\right)\Big|_{x=L} dz \tag{32}$$

where

$$\delta v_I = \delta R_n e^{-ik_n(x+L)}, \quad \frac{\partial\, \delta v_I}{\partial x} = -ik_n \delta R_n e^{-ik_n(x+L)} = -ik_n \delta v_I,$$

and

$$\delta v_{III} = \delta T_n e^{ik_n(x-L)}, \quad \frac{\partial\, \delta v_{III}}{\partial x} = ik_n \delta T_n e^{ik_n(x-L)} = ik_n \delta v_{III} \tag{33}$$

because

$$v_I = I_n e^{ik_n(x+L)} + R_n e^{-ik_n(x+L)}, \quad v_{III} = T_n e^{ik_n(x-L)}$$

Performing integration by parts and exploiting properties of the wave ansatz [Eqs. (16) and (17)] yield

$$\delta\mathcal{A} = \left\langle \left(-\rho\frac{\partial^2 v_{II}}{\partial t^2} + \mu\frac{\partial^2 v_{II}}{\partial x^2} + \mu\frac{\partial^2 v_{II}}{\partial z^2}\right)\delta v_{II}\right\rangle_{x,z,t}$$

$$+ \left[\left\langle \rho\frac{\partial v_{II}}{\partial t}\delta v_{II}\right\rangle_{x,z}\right]_{t_1}^{t_2} - \left\langle \mu_1\left(\frac{\partial v_{1_{II}}}{\partial z}\right)\delta v_{1_{II}}\Big|_{z=0}\right\rangle_{x,t}$$

$$+ \left\langle \mu_2\left(\frac{\partial v_{2_{II}}}{\partial z}\right)\delta v_{2_{II}}\Big|_{z\to\infty}\right\rangle_{x,t}$$

$$+ \left\langle \left[\mu_2\left(\frac{\partial v_{2_{II}}}{\partial x}n_x + \frac{\partial v_{2_{II}}}{\partial z}n_z\right)\right.\right.$$

$$\left.\left. - \mu_1\left(\frac{\partial v_{1_{II}}}{\partial x}n_x + \frac{\partial v_{1_{II}}}{\partial z}n_z\right)\right]\delta v_{1_{II}}\Big|_{z=\eta_{(x)}}\right\rangle_{x,t}$$

$$- \left\langle \mu_2\left(\frac{\partial \delta v_{2_{II}}}{\partial x}n_x + \frac{\partial \delta v_{2_{II}}}{\partial z}n_z\right)(v_{2_{II}} - v_{2_{II}})\Big|_{z=\eta_{(x)}}\right\rangle_{x,t}$$

$$+ \left\langle \left[\mu\frac{\partial v_I}{\partial x} - \mu\left(\frac{\partial v_{II}}{\partial x}\right)\right]\delta v_{II}\Big|_{x=x_1}\right\rangle_{z,t}$$

$$+ \left\langle \left[\mu\left(\frac{\partial v_{II}}{\partial x}\right) - \mu\left(\frac{\partial v_{III}}{\partial x}\right)\right]\delta v_{II}\Big|_{x=x_2}\right\rangle_{z,t}$$

$$- i\mu k_{n(-L)}\left\langle \delta v_I (v_I - v_{II})|_{x=x_1}\right\rangle_{z,t}$$

$$- i\mu k_{n(L)}\left\langle \delta v_{III}(v_{III} - v_{II})|_{x=x_2}\right\rangle_{z,t} \tag{34}$$

where

$$\langle f\rangle_{x,z,t} = \int_{t_1}^{t_2}\int_{x_1}^{x_2}\int_{0}^{\infty} f\, dx\, dz\, dt \tag{35}$$

is the space-time average of the integrand f. Note that in Eq. (34) δv_I, $\delta v_{1_{II}}$, $\delta v_{2_{II}}$, δv_{III} are arbitrary. Thus, the only way to impose $\delta\mathcal{A}$ identically to zero is by setting at each line of Eq. (34) the integrand of the space-time integral equal to zero. This yields the boundary value problem [Eqs. (1)–(3), (6)].

Appendix II. Matrix Coefficients

$$b_{ij} = -\left(\frac{1}{2}\right)e^{i(k_i - k_j)x}\left(F^1_{(ij)}\mu_1 + F^2_{(ij)}\mu_2\right)$$

$$c_{ij} = \frac{1}{2}e^{i(k_i-k_j)x}\left[\mu_1\left(F^1_{(ij_x)} - F^1_{(i_x j)} - \frac{\partial F^1_{(ij)}}{\partial x} + 2F^1_{(ij)}\Psi\right)\right.$$
$$\left. + \mu_2\left(F^2_{(ij_x)} - F^2_{(i_x j)} - \frac{\partial F^2_{(ij)}}{\partial x} + 2F^2_{(ij)}\Psi\right)\right]$$

$$d_{ij} = \frac{1}{2}e^{i(k_i-k_j)x}\left\{-\omega^2\left(\rho_1 F^1_{(ij)} + \rho_2 F^2_{(ij)}\right) + \mu_1\left[F^1_{(i_x j_x)}\right.\right.$$
$$\left. + F^1_{(i_z j_z)} - \frac{\partial F^1_{(i_x j)}}{\partial x} + \left(F^1_{(i_x j)} + \frac{\partial F^1_{(i,j)}}{\partial x} - F^1_{(ij_x)}\right)\Psi + F^1_{(ij)}\Phi\right]$$
$$+ \mu_2\left[F^2_{(i_x j_x)} + F^2_{(i_z j_z)} - \frac{\partial F^2_{(i_x j)}}{\partial x}\right.$$
$$\left.\left. + \left(F^2_{(i_x j)} + \frac{\partial F^2_{(ij)}}{\partial x} - F^2_{(ij_x)}\right)\Psi + F^2_{(ij)}\Phi\right]\right\}$$

where

$$\Psi = -ik_i + ix\frac{\partial k_i}{\partial x}$$

J. Eng. Mech. 2013.139:1158-1165.

$$\Phi = k_i^2 - i\frac{\partial k_i}{\partial x} - i\frac{\partial^2 k_i}{\partial x^2}x + 2k_i\frac{\partial k_i}{\partial x}x + \left(\frac{\partial k_i}{\partial x}\right)^2 x^2$$

$$F^d_{(n\,m)} = \int_0^\eta f^d_m(z,\eta) f^d_n(z,\eta)dz$$

$$F^d_{(n\,m_x)} = \int_0^\eta f^d_n(z,\eta)\frac{\partial}{\partial x} f^d_m(z,\eta)dz$$

$$F^d_{(n_x\,m)} = \int_0^\eta f^d_m(z,\eta)\frac{\partial}{\partial x} f^d_n(z,\eta)dz$$

$$F^d_{(n_x\,m_x)} = \int_0^\eta \frac{\partial}{\partial x} f^d_m(z,\eta)\frac{\partial}{\partial x} f^d_n(z,\eta)dz$$

$$F^d_{(n_z,m_z)} = \int_0^\eta \frac{\partial}{\partial z} f^d_m(z,\eta)\frac{\partial}{\partial z} f^d_n(z,\eta)dz$$

and

$$f_n(z,\eta) = \begin{cases} f^1_n(z,\eta) = 2\cos(\nu_1 z) & 0 \le z \le \eta \\ f^2_n(z,\eta) = 2\cos(\nu_1\eta)e^{-\nu_2(z-\eta)} & z \ge \eta \end{cases}$$

$$\nu_i = \sqrt{k_n^2 - \omega^2/\beta_1^i}$$

References

Aki, K., and Richards, P. G. (2002). *Quantitative seismology: Theory and methods*, 2nd Ed., University Sciences Books, Sausalito, CA.

Ben-Hador, R., and Buchen, P. (1999). "Love and Rayleigh waves in non-uniform media." *Geophys. J. Int.*, 137(2), 521–534.

Bignardi, S. (2011). "Complete waveform inversion approach to seismic surface waves and adjoint active surfaces," Ph.D. thesis, Earth Sciences Dept., Univ. of Ferrara, Ferrara, Italy.

Bignardi, S., Fedele, F., Yezzi, A. J., Rix, G. J., and Santarato, G. (2012). "Geometric seismic wave inversion by the boundary element method." *Bull. Seismol. Soc. Am.*, 102(2), 802–811.

Brebbia, C. A., Tellers, J. C. F., and Wrobel, L. C. (1984). *Boundary element techniques*, Springer-Verlag, Berlin.

Du, Z. (2002). "Waveform inversion for lateral heterogeneities using multimode surface waves." *Geophys. J. Int.*, 149(2), 300–312.

Gjevik, B. (1973). "A variational method for love waves in nonhorizonatally layered structures." *Bull. Seismol. Soc. Am.*, 63(3), 1013–1023.

Knopoff, L., and Mal, A. K. (1967). "Phase velocity of surface waves in the transition zone of continental margins." *J. Geophys. Res.*, 72(6), 1769–1776.

Lysmer, J., and Drake, L. A. (1971). "The propagation of love waves across nonhorizontally layered structures." *Bull. Seismol. Soc. Am.*, 61(5), 1233–1251.

Maupin, V. (1988). "Surface waves across 2-d structures: A method based on coupled local modes." *Geophys. J. Int.*, 93(1), 173–185.

Maupin, V. (1992). "Modelling of laterally trapped surface waves with application to Rayleigh waves in the Hawaiian swell." *Geophys. J. Int.*, 110(3), 553–570.

Maupin, V. (2007). "Introduction to mode coupling methods for surface waves." *Adv. Geophys.*, 48, 127–155.

Maupin, V., and Kennett, B. L. N. (1987). "On the use of truncated modal expansions in laterally varying media." *Geophys. J. Int.*, 91(3), 837–851.

Noyer, J. (1961). "The effect of variations in layer thickness on Love waves." *Bull. Seismol. Soc. Am.*, 51(2), 227–235.

Panza, G. F., Romanelli, F., and Vaccari, F. (2001). "Seismic wave propagation in laterally heterogeneous anelastic media: Theory and applications to seismic zonation." *Adv. Geophys.*, 43, 1–95.

Rutherford, S. R., and Hawker, K. E. (1981). "Consistent coupled mode theory of sound propagation for a class of nonseparable problems." *J. Acoust. Soc. Am.*, 70(2), 554–564.

Trefethen, L. N. (2000). *Spectral Methods in MATLAB*, SIAM, Philadelphia.

Tromp, J., and Dahlen, F. A. (1992). "Variational principles for surface wave propagation on a laterally heterogeneous earth—II. Frequency-domain JWKB theory." *Geophys. J. Int.*, 109(3), 599–619.

Virieux, J., Calandra, H., and Plessix, R. E. (2011). "A review of the spectral, pseudo-spectral, finite-difference and finite-element modelling techniques for geophysical imaging." *Geophys. Prospect.*, 59(5), 794–813.

Whitham, G. B. (1967). "Variational methods and applications to water waves." *Proc. R. Soc. London, Ser. A*, 299(1456), 6–25.

Whitham, G. B. (1974). *Linear and Nonlinear Waves*, Wiley, Chichester, U.K.

Wolf, B. (1970). "Propagation of Love waves in layers with irregular boundaries." *Pure Appl. Geophys.*, 78(1), 48–57.